Paper No.
7406

NACE INTERNATIONAL CORROSION 2016 CONFERENCE & EXPO

Modeling of Corrosion Mechanisms in the Presence of Quaternary Ammonium Chloride and Imidazoline Corrosion Inhibitors

J.M. Domínguez Olivo, B. Brown, S. Nesic
Institute for Corrosion and Multiphase Technology.
Ohio University
Athens, OH 45701

ABSTRACT

The mitigation of corrosion in carbon steel pipelines due to the addition of corrosion inhibitors has traditionally been described by using adsorption isotherms. Consequently, current models of corrosion mitigation by inhibitors are based on the use of adsorption isotherms to predict surface coverage, inhibitor efficiency and ultimately the corrosion rate as a function of inhibitor concentration. However, a coverage does not properly describe the underlying electrochemical mechanisms, nor can it predict the resulting change in corrosion potential. The goal of this research is to analyze and explain how the underlying electrochemical reactions are affected by the presence of adsorbed corrosion inhibitor and the shift in corrosion potential that occurs. Two CO_2 corrosion inhibitors are studied here: tail oil fatty acid / diehylenetriamine imidazoline and quaternary alkyl benzyl dimethyl ammonium chloride. A mechanistic model was developed based on electrochemical kinetics and by using a mitigation factor, θ, which accounts for the overall retardation in the anodic and cathodic reactions. It was found that the retardation of the electrochemical reactions affected by these inhibitor can be modeled by using a single parameter: surface coverage factor.

Key words: corrosion inhibitors, mechanistic model, mitigation.

INTRODUCTION

The oil and gas industry has long considered the use of corrosion inhibitors as an effective and affordable method to mitigate corrosion.[1] Most literature characterize inhibitor effectiveness through the use of a surface coverage factor.[2–4] A corrosion inhibitor is a chemical substance that significantly reduces the corrosion rate in certain environments when it is added in small concentrations[2]. Much of the knowledge about corrosion inhibition for specific environments has been obtained by simulating the operating field conditions in the laboratory and measuring the inhibition efficiency of different corrosion inhibitors[2–4]. Engineers have used inhibition efficiency to develop mathematical models based upon adsorption isotherms by assuming that the inhibitors cover the metal surface as a uniform thin film and this coverage is directly proportional to the inhibition efficiency[3,5–8] This approach to describing and modeling inhibitor effectiveness is helpful, but there is a need to develop a more mechanistic approach to modeling that requires a more detailed understanding of the adsorption and electrochemical mechanisms underlying corrosion inhibition.

The most widely accepted classification of corrosion inhibition mechanisms was proposed by Lorenz[9] and corroborated by the methodology proposed by Cao[10]. In this classification, the open circuit potential is the main parameter. There are three possible effects of the corrosion inhibitor:

Blockage effect: A surface blocking effect is present when an inert adsorbed species (a species which does not reduce or oxidize) covers a significant fraction of the corroding surface and thereby retards both cathodic and anodic kinetics equally, so the open circuit potential (corrosion potential, OCP) does not change significantly.

Preferential retardation of anodic or cathodic reaction: Preferential adsorption occurs when the corrosion inhibitor favorably adsorbs onto either the cathodic or the anodic sites affecting kinetics differently and this results in a change of the corrosion potential. The corrosion potential shifts into the positive direction when the inhibitor affect the anodic reaction more and shifts in the negative when the inhibitor affect the cathodic reaction preferentially.

Electrocatalytic effect: The corrosion inhibitor interferes with the electrochemical mechanism of the corrosion process and the Tafel slope of any given reaction may change. The open circuit potential may or may not change when an electrocatalytic effect is present.

However, this relatively easy to understand classification, based upon the change of the corrosion potential, is not helpful when the corrosion process is under mixed or mass transfer control.[11] This is because the adsorption of the corrosion inhibitor readily affects the charge transfer reactions (which are surface phenomena) but does not affect the diffusion of species (which is a “bulk” electrolyte phenomenon). The same holds true when corrosion is controlled by a slow homogenous chemical reaction rate, such as for example CO_2 hydration. Consequently, the change of the open circuit potential in CO_2 corrosion is not directly related to the retardation of the individual electrochemical reactions, as illustrated in the schematic in Figure 1. In that particle scenario, a positive shift on the corrosion potential is obtained even if it is assumed that the blockage effect produces equal retardation of the anodic and cathodic charge transfer reaction, what is at odds with the Lorenz/Cao classification, which would suggest that this is inhibitor retards the anodic reaction preferentially.

Many subsequent studies have used this methodology to interpret the effect of corrosion inhibitors on the change of the anodic and cathodic corrosion mechanisms [9,10,12,13]. However, this was not done rigorously and in most cases the overall effect of the corrosion inhibitor was loosely qualified as being “anodic” or “cathodic”, based upon the change of the corrosion potential[3,14–16]. However, as argued above, this may lead to incorrect conclusions about the inhibition mechanisms. In order to avoid such errors in the interpretation of results, the work presented below proposes a somewhat different methodology to qualify and quantify the retardation of corrosion due to the presence of an adsorbed corrosion inhibitor[17,18].

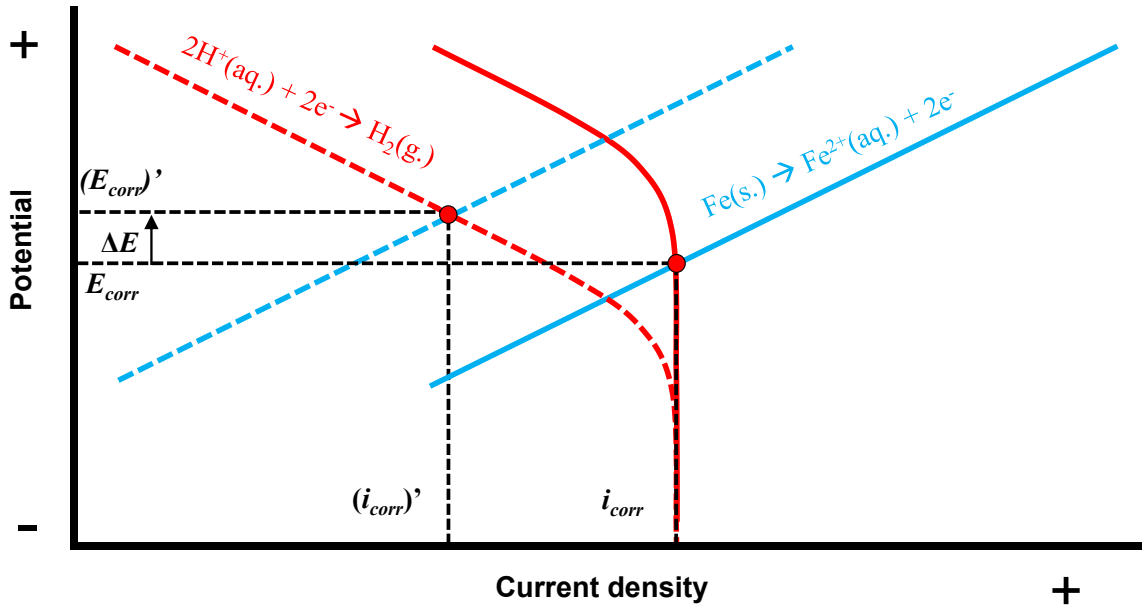

Figure 1: A hypothetical corrosion kinetics diagram illustrating the surface blockage effect when equal retardation of charge transfer processes is seen (both anodic and cathodic), but one that produces a net positive change of potential (ΔE) because the uninhibited cathodic reaction is under mass transfer control. Solid lines: uninhibited reactions. Dashed lines: inhibited reactions. E_{corr}: corrosion potential of uninhibited reactions, $(E_{corr})'$: corrosion potential of inhibited reactions, i_{corr} : corrosion current density of uninhibited reactions, $(i_{corr})'$: corrosion current density of inhibited reactions.

EXPERIMENTAL PROCEDURE

A three electrode electrochemical system was set up in a 2-liter glass cell and used to perform a series of experiments at 1 bar, pH 4 and 30 °C. In a 1 wt % NaCl solution. An API 5L X65 steel rotating cylinder electrode (RCE) at 1000 rpm was used as the working electrode, as shown in Figure 2. The composition of the steel is shown in Table 1. A platinum covered titanium mesh was used as the counter electrode and an Ag/AgCl reference electrode was used as the reference electrode connected with the cell using a Luggin capillary. Two different gases (N_2 or CO_2) were used for purging the system to remove dissolved oxygen and saturate the solution. The solution pH was measured using a glass electrode immersed directly in solution and maintained at pH 4.0±0.1 during each experiment.

Linear polarization resistance (LPR) was used to obtain corrosion rates by polarizing the working electrode ±5 mV from the corrosion potential (using B = 26 mV). Electrochemical impedance spectroscopy (EIS) was used for measuring solution resistance by employing an oscillating potential ±5 mV with respect to the corrosion potential and using a frequency range between 5mHz to 5KHz. Potentiodynamic polarization was applied at the end of each experiment at a rate of 1.25 mV/s in order to obtain information about the electrochemical mechanisms underlying corrosion (cathodic and anodic reactions). The cathodic curve was obtained by polarizing from the open circuit potential to approximately -0.5 V below. After waiting for the corrosion potential to return to the original open circuit potential, another potentiodynamic polarization was performed in the positive direction for +0.3 V, in order to obtain the anodic curve. Each potentiodynamic curve was corrected with the ohmic drop caused by the solution resistance to show the relevant current vs. voltage relationship.

Two different corrosion inhibitor packages were tested and analyzed: a quaternary alkyl benzyl dimethyl ammonium chloride based corrosion inhibitor (referred to as “quat” in the text below) and a tail oil fatty acid / diethylenetriamine (TOFA/DETA) imidazoline based corrosion inhibitor (referred to as

"imidazoline"). Concentrations were selected based on their respective critical micelle concentrations in a 1 wt% NaCl solution: 110 ppm v/v for the quat at 36 ppm v/v for the imidazoline. The formulation of the corrosion inhibitor packages is shown in Table 2 and the structure of the active components in the inhibitor packages are shown in Figure 3 and Figure 4. The experimental conditions are shown in Table 3.

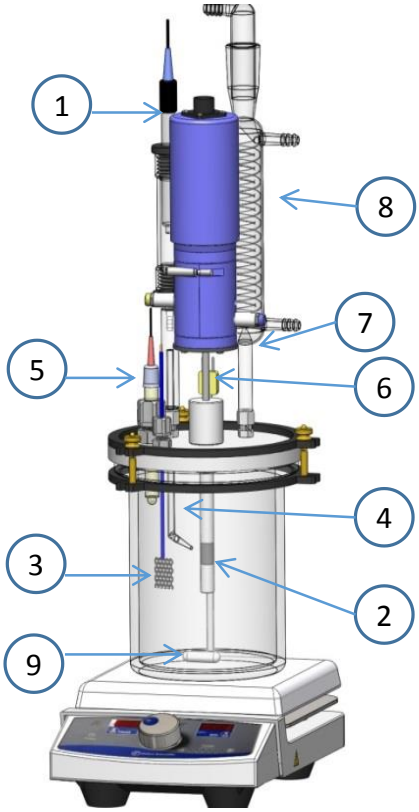

1. **Reference electrode (RE – Saturated Ag / AgCl)**
2. **Rotating Cylinder Electrode (WE)**
3. **Counter electrode (CE)**
4. **Luggin Capillary**
5. **pH meter**
6. **Thermocouple**
7. **Gas in**
8. **Gas out**
9. **Magnetic Stirrer**

Figure 2: Three electrode set up used to perform experiments.

Table 1: Chemical Composition of the X65 Steel Used as Working Electrode

Composition	Elements									
	Cr	Mo	S	V	Si	C	Ni	Mn	P	Fe
Weight %	0.14	0.16	0.009	0.047	0.26	0.13	0.36	1.16	0.009	Balance

Table 2: Chemical Composition of the Corrosion Inhibitor Packages

Description	Active ingredient	Components
Generic inhibitor	quaternary alkylbenzyl dimethyl ammonium chloride	24% Alkylbenzyl dimethyl ammonium chloride
		Balance water
Generic inhibitor	tail oil fatty acid / diethylenetriamine (TOFA/DETA) imidazoline	10% CH_3COOH
		13% $C_4H_9OCH_2CH_2OH$
		24% TOFA/DETA imidazoline
		Balance water

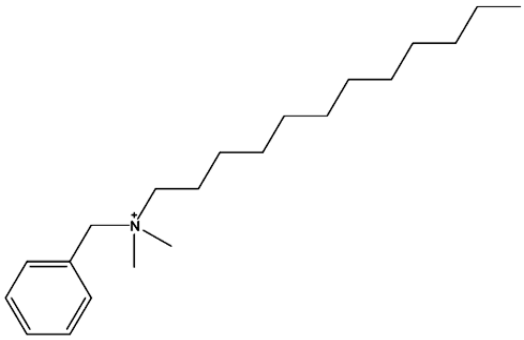

Figure 3: Structure of quaternary alkylbenzyl dimethyl ammonium chloride

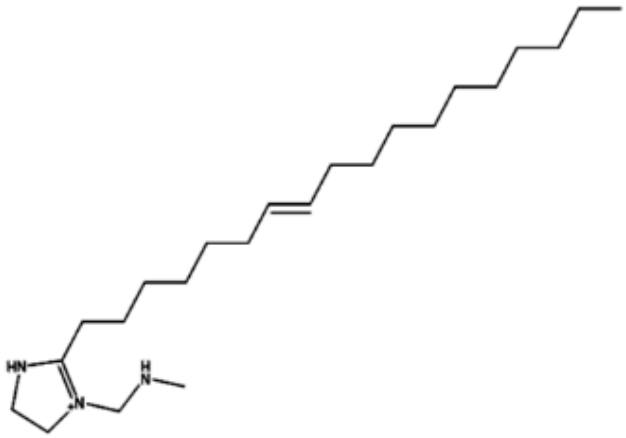

Figure 4: Structure of tail oil fatty acid / diethylenetriamine TOFA/DETA imidazoline.

Table 3: Experimental Conditions

Description	Parameters
Test material	API 5L X65
Working solution	1 wt% NaCl
Purged gas	N_2, 0.96 bar CO_2
Temperature	30 °C
pH	4
Corrosion inhibitors	none (baseline), quat, imidazoline
Test duration	2-12 hours (stabilization of corrosion rate)
Measurement methods	LPR, EIS, potentiodynamic polarization

RESULTS AND DISCUSSION

Corrosion mitigation efficiency

LPR corrosion rates over a 7-hour experimental time period for the environmental conditions defined in Table 3 are shown in Figure 5 and Figure 6. When the corrosion rate did not significantly change over time (less than ±0.01 mm/year between measurements), the corrosion mitigation efficiency was calculated. In order to calculate the corrosion mitigation efficiency (ε), Equation (1) was used:

$$\varepsilon = 1 - \frac{(CR)_\theta}{CR} \quad (1)$$

Where $(CR)_\theta$ is the corrosion rate of the system with corrosion inhibitor and CR represents the corrosion rate of the same system without the inhibitor present. The final corrosion rates and the corrosion mitigation efficiency are presented in Table 4. As it can be seen, the corrosion mitigation efficiency for the imidazoline corrosion inhibitor is very high in each condition tested (more than 97% in all cases) while the quat exhibits a low corrosion mitigation efficiency in either N_2 or CO_2 purged systems (75 and 86% respectively).

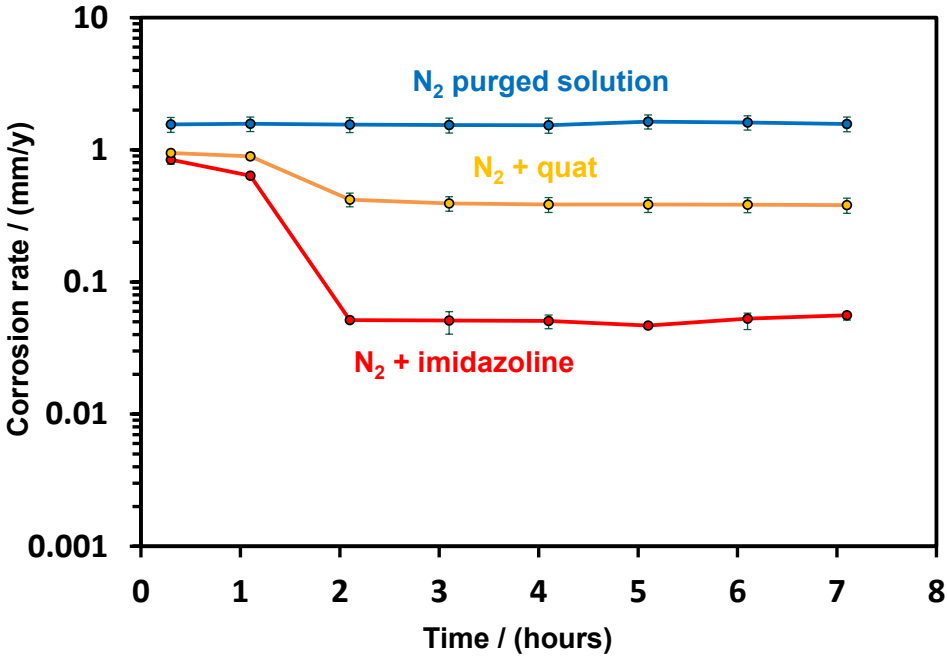

Figure 5: LPR measured corrosion rates over time for a N_2 purged system at 30°C, pH 4, RCE at 1000 rpm (B = 26 mV).

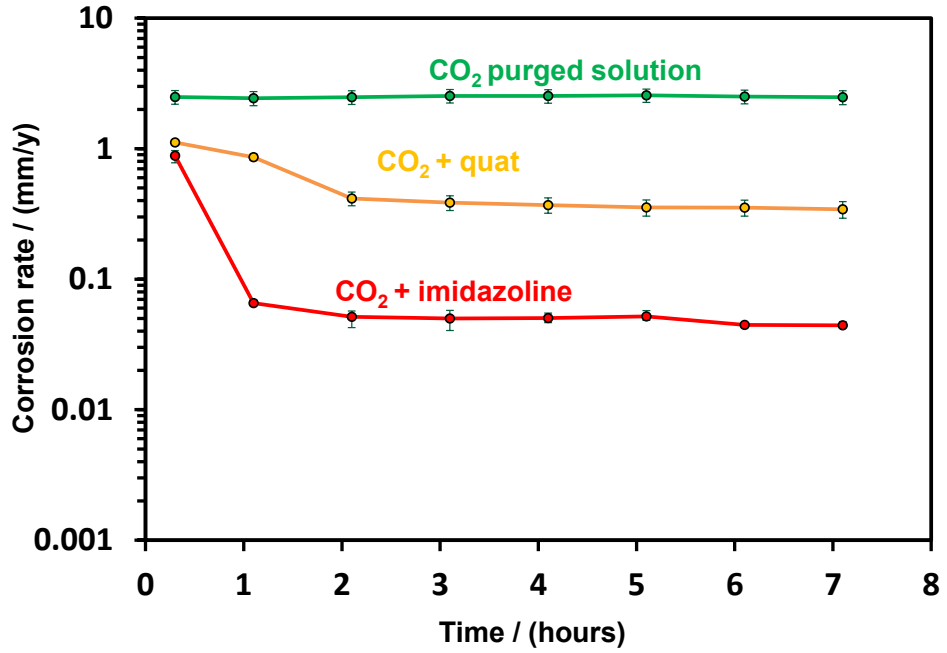

Figure 6: LPR measured corrosion rates over time for a 0.96 bar saturated system at 30°C, pH 4, RCE at 1000 rpm and. (B = 26 mV)

Table 4 : Final Corrosion Rate (mm/year) and Corrosion Mitigation Efficiency (ε) for Different Tests

Purge Gas	Blank (mm/year)	Corrosion Rates (mm/year)		Corrosion mitigation efficiency (%)	
		imidazoline	quat	imidazoline	quat
N_2	1.6 ± 0.1	0.05 ± 0.002	0.4 ± 0.05	97.5 ± 0.5	75.5 ± 0.5
CO_2	2.3 ± 0.2	0.05 ± 0.01	0.3 ± 0.05	97.0 ± 0.5	86.0 ± 0.5

Potentiodynamic polarization curves

The potentiodynamic sweeps for the N_2 purged solution are shown in Figure 7. The quat inhibitor does not lead to a significant change in the corrosion potential nor does it seem to change the corrosion mechanism, judging by the appearance of the potentiodynamic sweeps before and after addition of the inhibitor. The imidazoline corrosion inhibitor also does not significantly modify the corrosion potential, however, the mechanisms of the cathodic reaction seem to change from diffusion limiting current to pure charge transfer control.

When the same corrosion inhibitors are added to a CO_2 saturated solution (Figure 8), the situation changes. In the presence of quat corrosion inhibitor the open circuit potential changed significantly - about 50 mV (considerably more than the experimental error). From the potentiodynamic sweeps, this appears to be because the iron dissolution (anodic reaction) seems to be affected more, while the cathodic reaction is affected in a similar way as in the N_2 purged solution. On the other hand, the imidazoline-based corrosion inhibitor does not appear to significantly change the corrosion potential, while it seems to affect the both the cathodic and the anodic reaction proportionally, and in both cases much more that it did for a N_2 purged system.

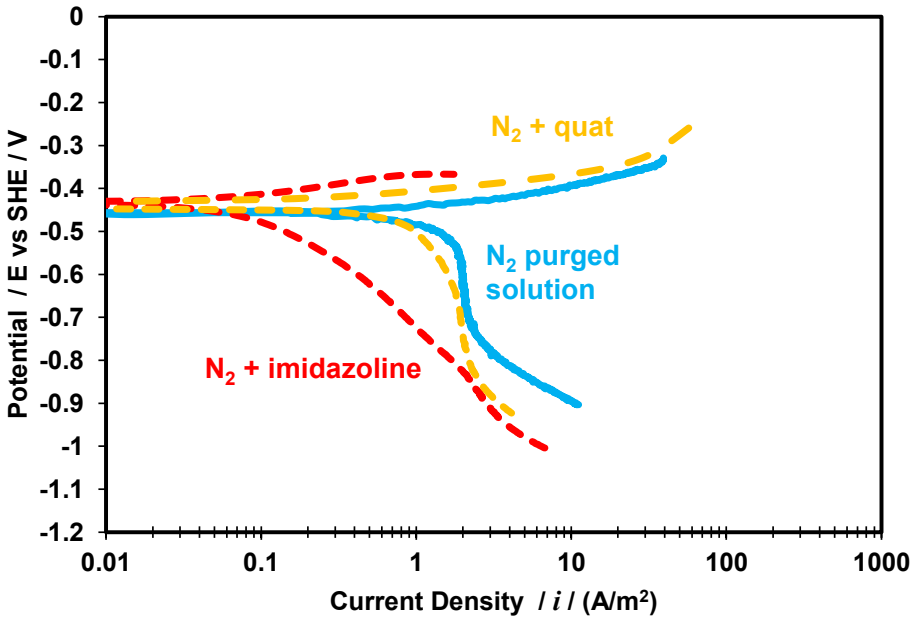

Figure 7: Potentiodynamic sweeps for a N_2 purged system at 30°C, pH 4, RCE at 1000 rpm. Solid blue line: baseline condition with no inhibitor; dashed orange line: after quat inhibitor added; dotted red line: after imidazoline inhibitor added.

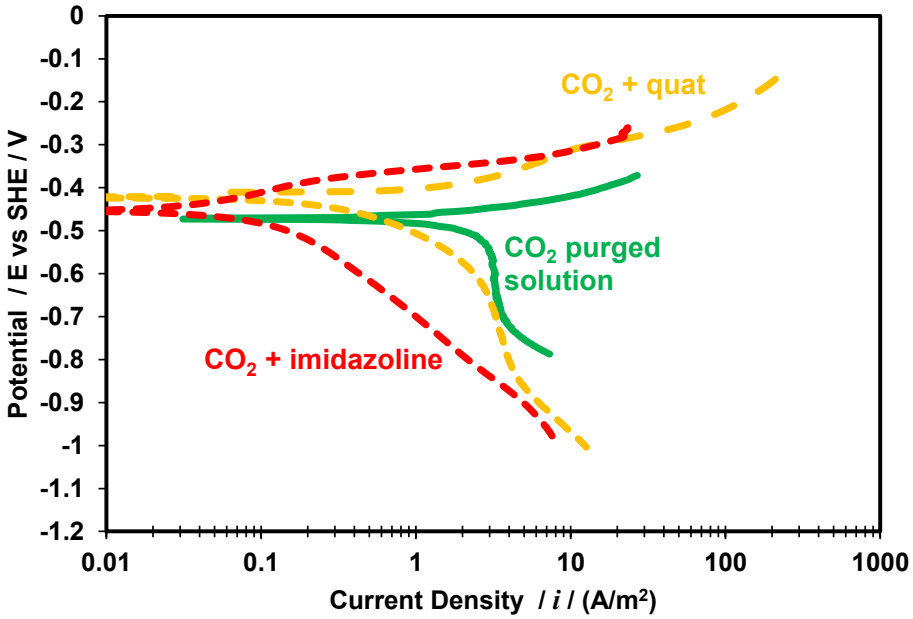

Figure 8: Potentiodynamic sweeps for a 0.96 bar CO_2 saturated system at 30°C, pH 4, RCE at 1000 rpm, and. Solid green line: baseline condition with no inhibitor; dashed orange line: after quat inhibitor added; dotted red line: after imidazoline inhibitor added.

Mechanistic model

In order to develop an analytical tool that can be used to investigate corrosion mechanisms, it is necessary to make some assumptions. In some previous corrosion inhibition studies[3,8–10], researchers have related the retardation of the corrosion current density (i_{corr}) with a corrosion surface coverage fraction by the inhibitor (θ) by assuming that the area covered by the inhibitor does not corrode at all while the surface which is not covered corrodes as if the inhibitor is not present[8]. This leads to simple relationship between the inhibition efficiency and surface coverage[9,10]:

$$\varepsilon = 1 - \frac{(CR)_\theta}{CR} = \theta \tag{2}$$

This allows substitution of the surface coverage (θ) for efficiency (ε) in Equation 2, along with substitution of corrosion current i_{corr} for CR, to develop Equation (3):

$$(i_{corr})_\theta = i_{corr}(1-\theta) \tag{3}$$

where:

$(i_{corr})_\theta$ is the corrosion current with surface coverage by an inhibitor (A/m^2).

i_{corr} is the corrosion current in the absence of inhibitor (A/m^2).

θ is the surface coverage fraction (with values from 0 to 1).

If we further assume that this surface coverage effect is not selective, we can postulate that the effective exchange current density for both the anodic and cathodic reactions are affected in the same way, leading to:

$$\left(i_0\right)_\theta = i_0\left(1-\theta\right) \tag{4}$$

where:

$\left(i_0\right)_\theta$ is the effective exchange current density affected by coverage of the inhibitor (A/m^2).

i_0 is the exchange current density in the absence of inhibitor (A/m^2).

This has been implemented in the electrochemical CO_2 corrosion model for both cathodic and anodic reactions previously proposed by Nesic and Zheng[17,18], including the buffering effect recently proposed by Remita[19]. For the iron dissolution reaction, that is under charge transfer control, this leads to a simple correction of the anodic current density, to include the effect of surface coverage, θ:

$$\left(i_{ct}^a\right)_\theta = \left(i_0^a\right)_\theta 10^{\frac{\eta_a}{b_a}} = \left(1-\theta\right) i_0^a \, 10^{\frac{\eta_a}{b_a}} \tag{5}$$

where:

$\left(i_{ct}^a\right)_\theta$ is the anodic charge transfer current density affected by coverage of the inhibitor (A/m^2).

$\left(i_0^a\right)_\theta$ is the effective anodic exchange current density affected by coverage of the inhibitor (A/m^2).

i_0^a is the anodic exchange current density in the absence of inhibitor (A/m^2).

η_a is the anodic overpotential: $\eta_a = E_{applied} - E_{rev}$

E_{app} is the applied potential (V).

E_{rev} is the reversible potential (V).

b_a is the anodic Tafel slope (V/decade).

For the cathodic reaction that has a limiting current density, only the charge transfer portion of the current is affected by the inhibitor coverage:

$$\frac{1}{\left(i^c\right)_\theta} = \frac{1}{\left(i_{ct}^c\right)_\theta} + \frac{1}{i_{\lim}} \tag{6}$$

where:

$\left(i^c\right)_\theta$ is the cathodic current density affected by coverage of the inhibitor (A/m^2).

(i_{lim}) is the limiting current density (A/m^2).

$\left(i_{ct}^c\right)_\theta$ is the cathodic charge transfer current density (A/m^2) given by:

$$\left(i_{ct}^c\right)_\theta = \left(i_0^c\right)_\theta 10^{-\frac{\eta_c}{b_c}} = \left(1-\theta\right) i_0^c \, 10^{-\frac{\eta_c}{b_c}} \tag{7}$$

where:

i_0^c is the cathodic exchange current density in the absence of inhibitor (A/m^2).

η_c is the cathodic overpotential: $\eta_a = E_{rev} - E_{applied}$

b_c is the cathodic Tafel slope (V/decade).

By comparing this model of corrosion kinetics with experimental data, it is possible to determine whether the assumption that was built in is actually correct, i.e. whether the corrosion inhibitor uniformly affects the kinetics of both the anodic or cathodic reaction or not.

Evaluation of the model

The aforementioned electrochemical model was compared to experimental data. Results indicate that the in the presence of the quat inhibitor one can use the same surface coverage factor θ = 0.75 for both reactions (anodic and cathodic) and for both the N_2 purged and CO_2 saturated solution and get a very good fit, as shown in Figure 9 and Figure 10. The success with use of the same coverage factor indicates that both cathodic and anodic reactions are equally affected; consequently there is no preferential adsorption on anodic sites, as it had been previously suggested by other researchers[3,15], even if the corrosion potential increased. The increase in potential can be attributed to the change of the cathodic process control from limiting current to charge-transfer control, after the inhibitor was added, similarly as was hypothesized in Figure 1. Furthermore, the fact that the same coverage factor was used for both the N_2 purged and CO_2 saturated systems suggests that the adsorption and inhibition by the quat corrosion inhibitor was not affected by the presence of CO_2.

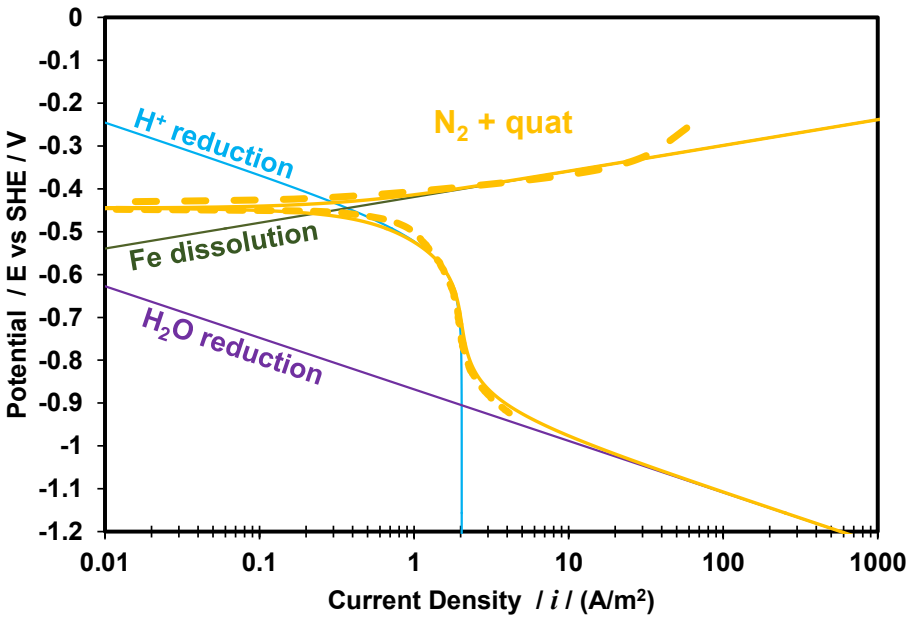

Figure 9: Comparison of predicted potentiodynamic sweeps including surface coverage factor θ =0.75 for a N_2 purged system at 30°C, pH 4, RCE at 1000 rpm. Dashed orange line: experimental results; solid orange line: model prediction.

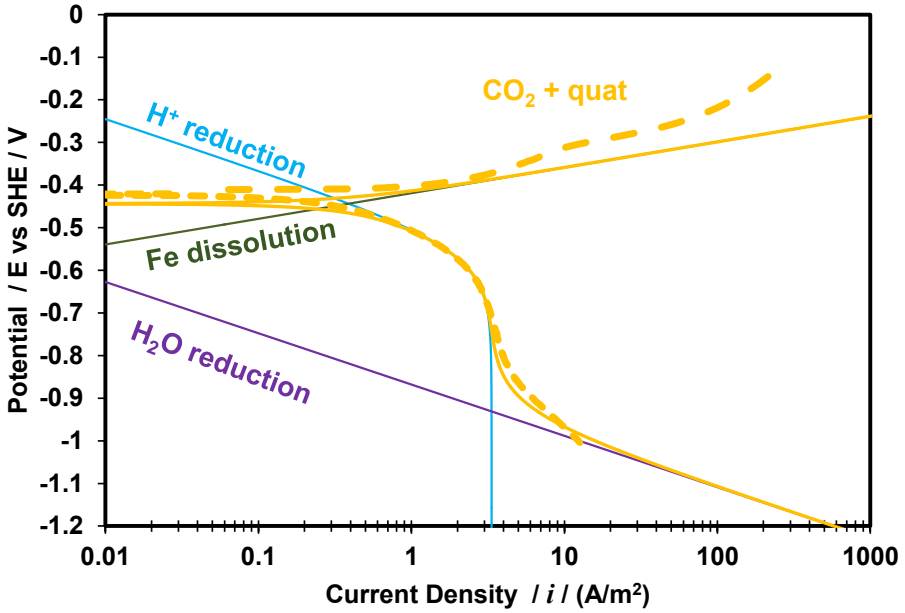

Figure 10: Comparison of predicted potentiodynamic sweeps including surface coverage factor θ =0.75 for a 0.96 bar CO_2 saturated system at 30°C, pH 4, RCE at 1000 rpm. Dashed orange line: experimental results. Solid orange line: model prediction.

Applying the same methodology for the imidazoline based corrosion inhibitor, and by using θ = 0.97, the results of comparing the calculated and measured potentiodynamic sweeps are shown in Figure 11 and Figure 12. Again, it can be concluded that the corrosion potential and corrosion mechanisms were predicted reasonably well by a single surface coverage factor, suggesting that this corrosion inhibitor also does not exhibit any preferential effect. However, there seem to be a deviation of the cathodic reaction from the expected behavior, particularly at higher overpotentials.

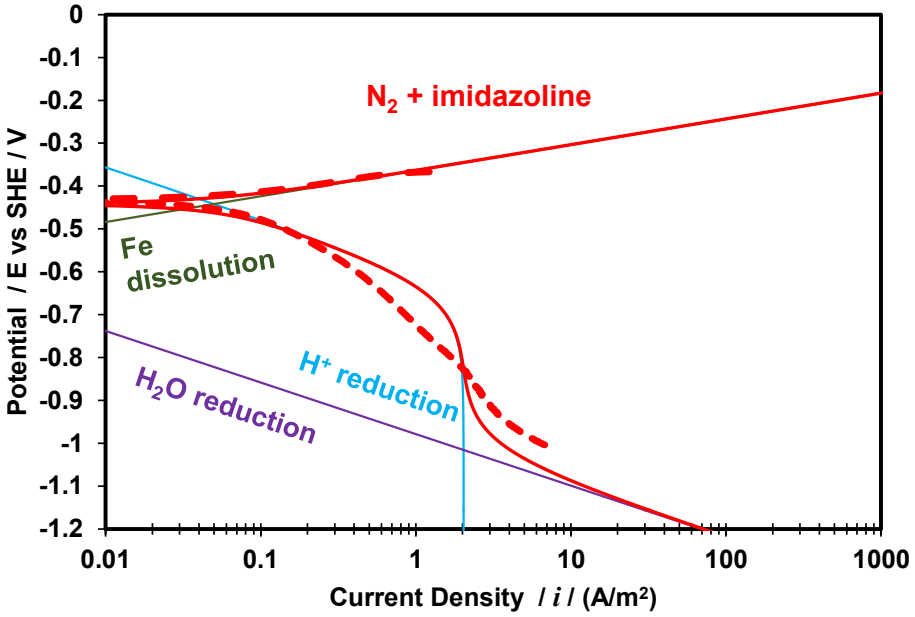

Figure 11: Comparison of predicted potentiodynamic sweeps including surface coverage factor θ =0.97 for a N_2 purged system at 30°C, pH 4, RCE at 1000 rpm. Dashed red line: experimental results; solid red line: model prediction.

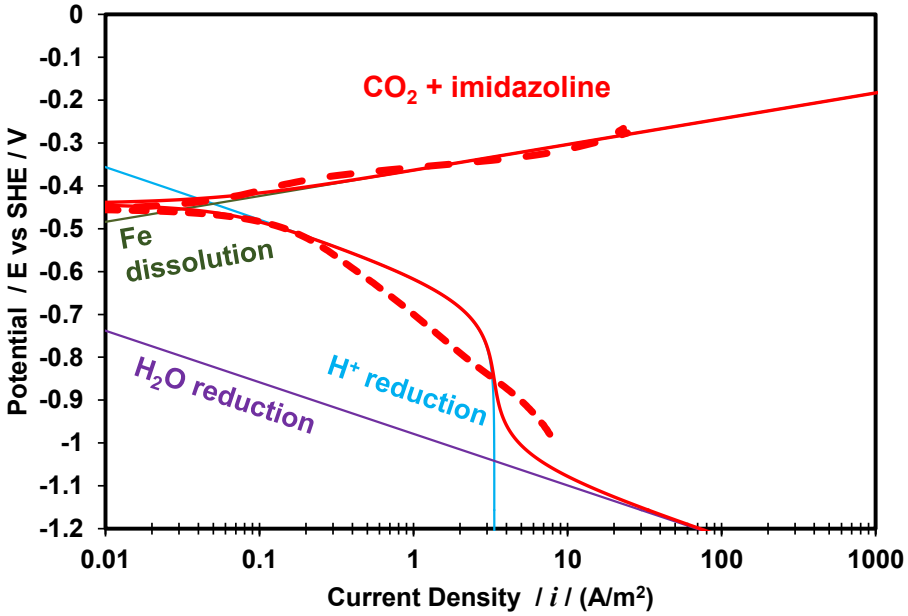

Figure 12: Comparison of predicted potentiodynamic sweeps including a surface coverage factor θ =0.97 for a 0.96 bar CO_2 saturated system at 30°C, pH 4, RCE at 1000 rpm. Dashed red line: experimental results; solid red line: model prediction.

Finally, in terms of corrosion rate and open circuit potential, this analytical tool can predict the corrosion rate and the open circuit potential of CO_2 and N_2 purged inhibited systems at pH 4 with reasonable accuracy, as shown in Table 5 and Table 6.

Table 5: Comparison of Prediction of Corrosion Rate by the Mechanistic Model

System	imidazoline (experimental) mm/yr	imidazoline (model) mm/yr	quat (experimental) mm/yr	quat (model) mm/yr
N_2	0.05 ± 0.002	0.07	0.4 ± 0.05	0.5
CO_2	0.05 ± 0.01	0.07	0.3 ± 0.05	0.5

Table 6: Comparison of Prediction of Corrosion Potential by the Mechanistic Model

System	imidazoline (experimental) mV vs SHE	imidazoline (model) mV vs SHE	quat (experimental) mV vs SHE	quat (model) mV vs SHE
N_2	-446 ± 5	437	-430± 5	-445
CO_2	-453 ± 5	437	-422 ± 5	-443

CONCLUSIONS

An analytical tool was developed that can be used to quantify the change in electrochemical corrosion kinetics due to the presence of a corrosion inhibitor. When applied to systems involving a quaternary ammonium chloride inhibitor and an imidazoline inhibitor, it was found that:

1. There was no preferential adsorption of either of the inhibitors on the electrode surface and the same corrosion mitigation factor, θ, could be used to model the retardation effect on the anodic and cathodic reaction.
2. The change of the corrosion potential following inhibition cannot be used as a meaningful indicator of the mechanism of corrosion inhibition, and its preferential nature.
3. The model can predict the corrosion rate and the open circuit potential in CO_2 and N_2 purged inhibited systems at pH 4 with reasonable accuracy.
4. A deviation of Tafel slopes is seen in potentiodynamic cathodic sweeps for the imidazoline-based inhibited at large overpotentials, which was not accounted for.

REFERENCES

1. D.A. Jones, *Principles and prevention of corrosion*, MacMillan, New York, 1996. p. 586.

2. S. Papavinasam, Corrosion Inhibitors, in: R.W. Revie (Ed.), Uhlig's Corros. Handb., Second Edi, Ottawa, 2000: pp. 1089–1105.

3. S. Nešić, W. Wilhelmsen, S. Skjerve, S.. Hesjevik, "Testing of inhibitors for CO2 corrosion using the electrochemical techniques," *Proc. 8th Eur. Symp. Corros. Inhib*. (8 SEIC). 10 (1995): pp. 1163–1192.

4. V.S. Sastri, *Green Corrosion Inhibitors*, 2nd ed., John Wiley & Sons, Hoboken, NJ, USA, 2011. p. 310.

5. D.M. Bastidas, P.P. Gómez, E. Cano, "The isotherm slope . A criterion for studying the adsorption mechanism of benzotriazole on copper in sulphuric acid," *Rev. Metal*. 1 (2005): pp. 98–106.

6. S. Paria, K.C. Khilar, "A review on experimental studies of surfactant adsorption at the hydrophilic solid-water interface," *Adv. Colloid Interface Sci*. 110 (2004): pp. 75–95.

7. R. Atkin, V.S.J. Craig, E.J. Wanless, S. Biggs, "Mechanism of cationic surfactant adsorption at the solid-aqueous interface," *Adv. Colloid Interface Sci.* 103 (2003): pp. 219–304.

8. L.M. Vracar, D. Drazic, "Adsorption and corrosion inhibitive properties of some organic molecules on iron electrode in sulfuric acid," *Corros. Sci.* 44 (2002): pp. 1669–1680.

9. W.J. Lorenz, F. Mansfeld, "Interface and Interphase Corrosion Inhibition," *Electrochim. Acta.* 31 (1985): pp. 467–476.

10. C. Cao, "On Electrochemical Techniques For Interface Inhibitor Research," *Corros. Sci.* 38 (1996): pp. 2073–2082.

11. S. Nešić, "Key issues related to modelling of internal corrosion of oil and gas pipelines – A review," *Corros. Sci.* 49 (2007): pp. 4308–4338.

12. M.A. Veloz, I.G. Martínez, "Effect of Some Pyridine Derivatives on the Corrosion Behavior of Carbon Steel in an Environment Like NACE TM0177," *Corros. Sci.* 62 (2006): pp. 283–292.

13. M.A. Veloz, I. Gonzalez, "Electrochemical study of carbon steel corrosion in buffered acetic acid solutions with chlorides and H_2S," *Electrochim. Acta.* 48 (2002): pp. 135–144.

14. T. Vasudevan, S. Muralidharan, S. Alwarappan, S.V.K. Iyer, "The influence of N-hexadecyl benzyl dimethyl ammonium chloride on the corrosion of mild steel in acids," *Corros. Sci.* 37 (1995): pp. 1235–1244.

15. Y.P. Khodyrev, E.S. Batyeva, E.K. Badeeva, E.V. Platova, L. Tiwari, O.G. Sinyashin, "The inhibition action of ammonium salts of O,O′-dialkyldithiophosphoric acid on carbon dioxide corrosion of mild steel," *Corros. Sci.* 53 (2011): pp. 976–983.

16. G. Zhang, C. Chen, M. Lu, C. Chai, Y. Wu, "Evaluation of inhibition efficiency of an imidazoline derivative in CO_2-containing aqueous solution," *Mater. Chem. Phys.* 105 (2007): pp. 331–340.

17. M. Nordsveen, S. Nešić, "A Mechanistic Model for Carbon Dioxide Corrosion of Mild Steel in the Presence of Protective Iron Carbonate Films — Part 1 : Theory and Verification," *Corros. Sci.* 59 (2003): pp. 443–456.

18. Y. Zheng, B. Brown, S. Nešić, "Electrochemical Study and Modeling of H_2S Corrosion of Mild Steel," *Corros. Sci*. 70 (2014): pp. 351–365.

19. E. Remita, B. Tribollet, E. Sutter, V. Vivier, F. Ropital, J. Kittel, "Hydrogen evolution in aqueous solutions containing dissolved CO_2: Quantitative contribution of the buffering effect," *Corros. Sci.* 50 (2008): pp. 1433–1440.